InSAR Image Denoising Filter for Accurate DEM Generation

M. S. Hamid, *Member, IEEE* and M. Safy, *Member, IEEE*

Abstract—**InSAR image noise has a great effect on the efficiency of the phase unwrapping process and consequently the correct generation of the digital elevation model (DEM). However, phase unwrapping can be easier and more efficient by excellent interferometric phase image filtering which can be achieved by high noise reduction, perfect preservation of the image detail, and decreasing the number of residues. In this paper, a grey-scale soft morphological filter is optimized using the genetic algorithm and used to filter out the interferometric phase image noise. The filter parameters are optimized to achieve an optimum balance between the amount of noise reduction and the degree of preservation of the image detail. Simulated and real interferograms are employed to evaluate the performance of the optimized filter. The evaluation is based on both objective and subjective measures. The results demonstrate that the proposed filter achieves high noise reduction with perfect image detail preservation and very small number of residues. This outstanding performance guarantees efficient phase unwrapping and hence accurate DEM generation. The results show also that the filter outperforms other traditional filters used for denoising interferogram images.**

Index Terms—InSAR, interferogram, soft morphological filter (SMF), genetic algorithm (GA).

I. Introduction

INTERFEROMETRIC synthetic aperture radar (InSAR) imaging proved to be a very precise technique for developing a high resolution digital elevation model (DEM) of a terrain's surface [1]. Phase unwrapping is considered the most critical step in the DEM generation process and the accuracy of the generated DEM highly depends on this step [1]. However, the interferogram noise has a great influence on the success of the phase unwrapping process [2]. So to facilitate the phase unwrapping process and also to get accurate DEM, an efficient interferogram noise reduction must be performed. This can be accomplished by high reduction of the interferogram image noise with excellent preservation of the image detail structures such as the edges of phase fringes. Many algorithms are proposed in the literature in order to achieve a high noise reduction and in the same time good preservation of the interferogram image detail.

Manuscript received xxx;

M. S. Hamid is with the Department of Electronic Engineering, Military Technical College, Cairo 11766, Egypt (e-mail: mhasan@mtc.edu.eg).

M. Safy is with the Department of Electronic Engineering, Egyptian Academy for Engineering and Advanced Technology, Cairo 1754, Egypt (e-mail: msafy@eaeat.edu.eg).

Frost [3] proposed an adaptive filter, which is an exponentially-weighted averaging filter, in order to remove SAR speckle noise. The filter replaces the pixels of interest with a weighted sum of the values within the moving window. Although the filter achieves good reduction of the image noise it blurs the edges in the image which makes it practically unacceptable. Balan [4] developed an adaptive filter that chooses the window size and detects the noise, either clustered or isolated. Li [5] presented a patch-based adaptive filter and Chao [6] proposed a refined filter that combines Lee adaptive InSAR filter and the sigma filter. Qiu [7] proposed a local adaptive median filter which uses local statistics to detect SAR speckle noise and replace it with a local median value. However, the filter performance is not optimum because the window size is selected experimentally. Chen [8] modified a nonlinear filter to denoise the SAR interferogram and used a pyramid technique to restore the texture from the noisy term. The main drawbacks of this filter are the iterative restoration of the wiped off texture and the long processing time.

On the other hand, Feng [9] introduced a vector filtering technique for filtering interferometric phase images. The technique is based on the mapping of the interferogram image into its cosine and sine components. Then the two components are filtered by average filter and the phase image is reconstructed by inverse mapping from vector to single variable. Although the filter achieved high noise reduction with good preservation of the image detail, the filter failed to perfectly reconstruct the edges of phase fringes. Meng [10] proposed a new method that separates the interferogram components into high frequency part and low frequency part. Although the method is efficient in noise reduction but it is poor in reducing the number of residues so it is not suitable for DEM generation. Lin [11] tried to enhance the nonlocal (NL) filtering using an advantage of higher order singular value decomposition, but the preservation of the interferogram texture needs two NL methods in the complicated area. Bian [12] proposed two InSAR phase filtering techniques (PFWPSDE and PFUWSDE) in the wavelet domain, the PFUWSDE is efficient in InSAR applications but needs a long processing time and faces some problems with high density interferogram fringes. Li [13] proposed an efficient filtering method based on the combination between the empirical mode decomposition (EMD) and the Hölder exponent adjustment but with a long consumption time.

It is clear from the above discussion that, it is not common for a filtering technique to achieve high noise reduction with the perfect preservation of the interferogram image detail. Also, the performance of the filtering process does not always guarantee the remaining of small number of residues in the filtered image.

It is also obvious that many of the state of the art algorithms are computationally exhaustive and take long processing time.

In this paper, a grey-scale soft morphological filter (SMF) is optimized, using the genetic algorithm (GA), and used to filter out the interferometric phase image noise. The filter parameters are optimized to achieve an optimum balance between the amount of noise reduction and the degree of preservation of the interferometric phase image detail.

The rest of this paper is organized as follows. Section II presents a detailed explanation of the design of the proposed filter. Performance evaluation of the optimized soft morphological filter for filtering out the interferogram image noise is introduced in section III. Section IV demonstrates the results of applying the proposed filter and other three filters, used for interferogram image noise reduction, to simulated as well as real interferometric phase images. A discussion of the results is also introduced. A conclusion is given in section V.

II. DEIGN OF THE PROPOSED FILTER

This section reviews the theoretical principles of soft morphological filters and explains how the SMF's overall structuring function, rank, and soft morphological operations are optimized using the GA.

A. Soft Morphological Filters

Soft morphological filters are a class of structural nonlinear filters [14] which are also known as order statistics filters. SMFs are based on weighted order statistics which makes them more tolerant to small variations in the shapes of the objects in the image to be filtered than other nonlinear filters.

The two basic soft morphological operations are soft dilation and soft erosion. Based on these operations, soft closing and soft opening are defined [14]. The structuring system of the filter has three parameters a (hard center), b (structuring function), and r (order index). A is the support of the hard center and $b\backslash a$ is the soft boundary. $B\backslash A$ is the support of the soft boundary.

Grey-scale soft dilation of a signal f is defined as:

$f \oplus [b,a,r](x)$ = the r^{th} largest value of the multiset

$$\{r \diamond (f(x-\alpha)+a(\alpha))\} \cup \{(f(x-\beta)+b(\beta))\} \quad (1)$$

where $\alpha \in A$ and $\beta \in B\backslash A$.

$$n \diamond x = \overbrace{x,\dots,x}^{n\ times} \quad (2)$$

Grey-scale soft erosion of a signal f is defined as:

$f \ominus [b,a,r](x)$ = the r^{th} smallest value of the multiset

$$\{r \diamond (f(x-\alpha)+a(\alpha))\} \cup \{(f(x-\beta)+b(\beta))\} \quad (3)$$

where $\alpha \in A$ and $\beta \in B\backslash A$.

B. Filter Optimization

The design of the SMF requires determining the overall dimensions of the structuring function support of the hard center and soft boundary, the possible range of the repetition parameter, and the choice and maximum length of the soft morphological operations. The GA [15] is used for the optimization of the SMF to be able to optimize all these filter parameters which have such large search space. So, The GA searches for any 2_D grey scale soft morphological filter with a flat structuring function, a repetition parameter, and a combination of the soft morphological operations: soft erode, soft dilate, soft opening, and soft closing.

The idea behind optimizing the SMF using a flat structuring element is that the values of the interferogram are not altered to have good phase unwrapping and hence accurate DEM generation. As shown in Fig. 1, the overall size of the structuring function of the SMF is 7 × 7.

The hierarchical GA is used for the formation of the chromosome of the parameters of the SMF such that the structuring function's hard center and soft boundary, repetition parameter, and sequence of soft morphological operations are encoded into a chromosome and the structuring function genes are used to control the genes of the hard center and soft boundary of the SMF.

The fitness function of the GA is based on two conflicting objectives: mean absolute error (MAE) which measures the amount of noise reduction and image detail-preserving coefficient IDPC [9] which indicates the degree of image detail preservation. The fitness function is formulated as follows:

$$\text{Fitness} = \alpha_1 \text{Fit}_{\text{MAE}} + \alpha_2 \text{Fit}_{\text{IDPC}} \quad (4)$$

where $\alpha_1 = \alpha_2 = 0.5$ and,

$$\text{Fit}_{\text{MAE}} = 1 - (\text{MAE} / \text{MAE}_{\text{max}}) \quad (5)$$

MAE is the mean absolute error between the clean and filtered interferometric phase images and MAE_{max} is the maximum possible value of the MAE. Fit_{IDPC} is the correlation coefficient between the clean and filtered interferometric phase images. The parameters of the SMF are optimized by maximizing the fitness function in Equation (4) using the GA.

0	*	0	0	0	*	0
*	*	*	0	*	*	*
0	0	*	*	*	0	0
0	0	*	*	*	0	0
0	0	*	*	*	0	0
*	*	*	0	*	*	*
0	*	0	0	0	*	0

Fig. 1 Structuring function of the optimized SMF. "*" refers to a position that is out of the support of the structuring function.

The application of the optimized SMF (OSMF) to the interferometric phase image is carried out by first transforming the image into its cosine and sine components then the two components are filtered by the OSMF and finally the interferometric phase image is reconstructed back from its two filtered components.

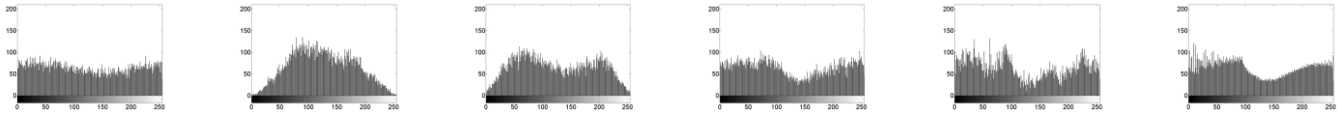

Fig. 2 Histogram of filtered simulated interferogram from left to right: Noisy, Frost, LAMF, VF, OSMF, and clean.

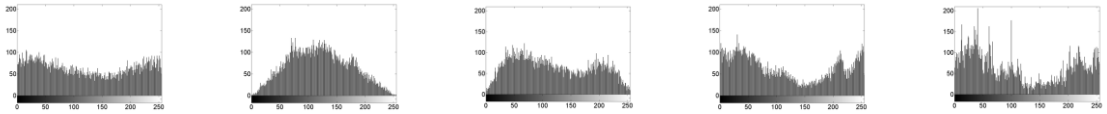

Fig. 3 Histogram of filtered sector of real interferogram from left to right: Noisy, Frost, LAMF, VF, and OSMF.

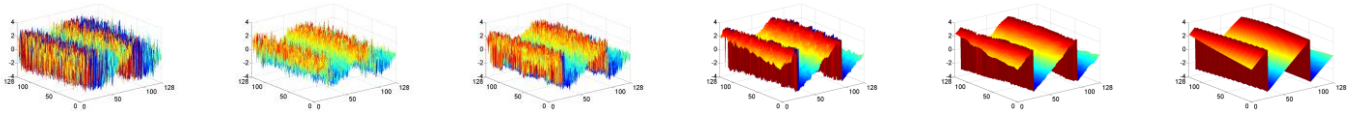

Fig. 4 Mesh of filtered simulated interferogram from left to right: Noisy, Frost, LAMF, VF, OSMF, and clean.

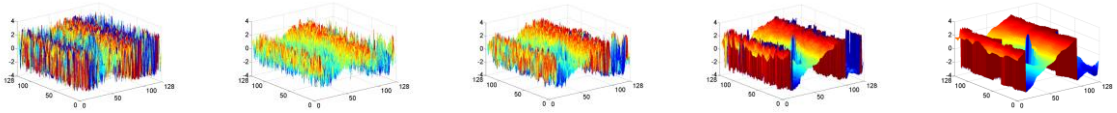

Fig. 5 Mesh of filtered sector of real interferogram from left to right: Noisy, Frost, LAMF, VF, and OSMF.

It is clear from Equation (1) and Equation (3) that the soft morphological operations require simple mathematics which can be easily calculated. Hence, most of the processing time is consumed in the optimization of the SMF and this is the drawback of the genetic algorithm. However, the application of the optimized filter to the interferometric phase image does not take long time which makes the filter very promising for filtering the huge InSAR image data.

The maximization of the fitness function in Equation (5) using the GA requires a clean version of the interferogram image. So, a model for the real interferogram image is constructed using a simulated interferogram. The simulated interferogram model and its real counterpart are shown in Fig. 6 and Fig. 7, respectively. The interferogram image model is created by selecting a region from the real interferogram image of the SAR pairs of ERS-1/2 tandem mode single look complex images shown in Fig. 8(a). Then a simulated interferogram, which has the same size and characteristics of the real interferogram image region, is created. The interferometric phase images of the two interferograms have very near characteristics in terms of their histogram distributions as shown in Fig. 2 and Fig. 3 and phase image variations as shown in Fig. 4 and Fig. 5. The interferometric phase image model and its clean version shown in Fig. 6 are used as training images for the GA.

The structuring function of the OSMF is shown in Fig. 1. The overall size of the structuring function is 7×7 and The filter has order index r = 14 and soft morphological operations: soft opening soft dilate soft dilate.

III. Performance Evaluation

The simulated interferogram image model is used for the evaluation of the performance of the OSMF and other three filters which are Frost filter [5], local adaptive median filter (LAMF) [7], and vector filtering (VF) [9]. This is carried out by using the objective measures demonstrated in Table I and also by the visual inspection of the filtered interferograms which are shown in Fig. 4 and Fig. 6. Also, the interferogram of SAR pairs of ERS-1/2 tandem mode single look complex images are used for the evaluation of the performance of the four filters. This is carried out by using the objective measures demonstrated in Table II and Table III and also by the visual inspection of the filtered interferometric phase images which are shown in Fig. 5, Fig. 7, and Fig. 8.

The four filters are compared in terms of MAE, MSE, Mean, IDPC [9], equivalent number of looks (ENL) [16], and number of residues (No_Res) [11]. MAE, MSE, and Mean measure the accuracy of the filtering process such that they show how much the values of the filtered interferogram image are near to the values of the clean one.

The ENL indicates the degree of reduction of the interferometric phase image noise. The larger the value of the ENL the higher the reduction of the image noise [13]. The No_Res estimates the degree of success of the unwrapping process. The smaller the number of the residues the better the efficiency of the unwrapping process and hence the higher the accuracy of the generated DEM. ENL and No_Res are important measures for the evaluation of the filter performance using real interferogram as they do not need reference (clean) interferogram images in their calculations.

IV. Results and Discussion

As explained in the previous section, the performance of the OSMF is evaluated using simulated and real interferogram images. The evaluation is based on both objective and subjective measures. The performance of the OSMF is also compared to three other filters used for denoising the interferometric phase images.

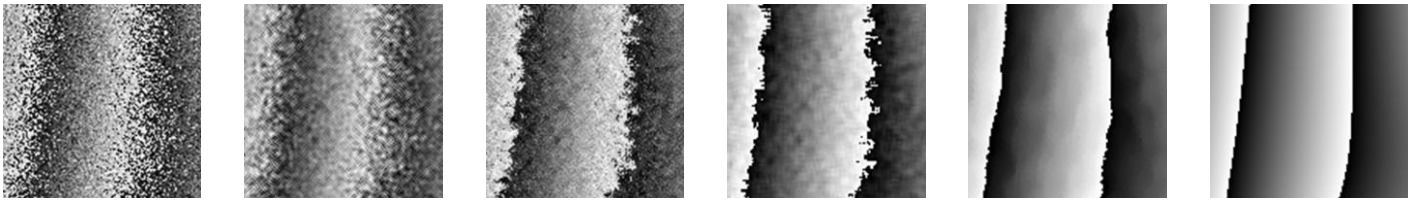

Fig. 6 Filtering results of simulated interferogram from left to right: Noisy, Frost, LAMF, VF, OSMF, and clean.

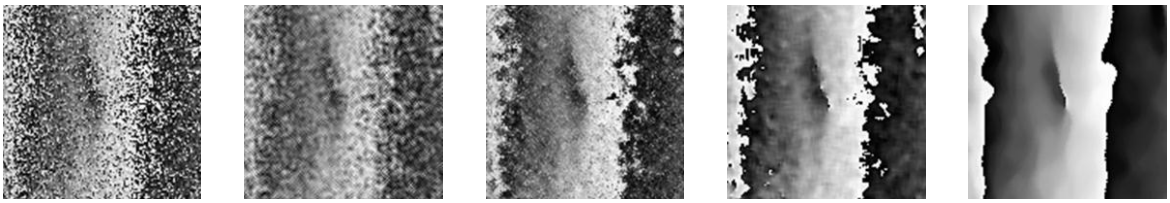

Fig. 7 Filtering results of sector of real interferogram from left to right: Noisy, Frost, LAMF, VF, and OSMF

TABLE I
PERFORMANCE COMPARISON FOR FILTERING SIMULATED INTERFEROGRAM

Evaluation Parameter	Clean	Noisy	Frost	LAMF	VF	OSMF
MAE	-	-	1.0763	0.7547	0.3503	0.1774
MSE	-	-	2.414	1.5759	1.1552	0.5845
Mean	0.1389	0.092	0.0636	0.0992	0.0926	0.1858
IDPC	-	-	0.5962	0.7617	0.8439	0.9219
ENL	69.4	6.7	24.0	36.8	57.8	66.4
No_Res	-	1237	520	428	0	0

TABLE II
PERFORMANCE COMPARISON FOR FILTERING REGION OF REAL INTERFEROGRAM

Evaluation Parameter	Noisy	Frost	LAMF	VF	OSMF
Mean	-0.1333	-0.1738	-0.2114	-0.3015	-0.3440
ENL	7.3	24.1	42.3	75.4	78.4
No_Res	2191	520	440	25	2

TABLE III
PERFORMANCE COMPARISON FOR FILTERING REAL INTERFEROGRAM

Evaluation Parameter	Noisy	Frost	LAMF	VF	OSMF
Mean	0.2404	0.2404	0.3381	0.4376	0.4021
ENL	8.0	28.4	32.1	65.4	96.0
No_Res.	171336	20906	18561	4478	192

A. Simulated Interferogram

The simulated interferogram model and its clean version are used for the evaluation of the performance of the OSMF and the other three filters which are Frost, LAMF, and VF. The results are demonstrated in Table I, Fig. 4, and Fig. 6.

Table I shows that the OSMF gives the lowest values for MAE and MSE which means that the filtered interferometric phase image is very close to the clean one and that leads to accurate DEM reconstruction. Also, the OSMF has the highest value for the ENL which indicates high reduction of the interferometric phase image noise and this is also clear in the smooth areas in Fig. 4 and Fig. 6. The OSMF gives the highest value for the IDPC which means perfect preservation of the interferometric phase image detail and this is clear from the perfect reconstruction of the edges of the phase fringe in Fig. 4 and Fig. 6. The OSMF gives zero number of residues, as demonstrated in Table I, and this leads to efficient phase unwrapping and hence accurate DEM generation. The results show also that the OSMF achieves perfect preservation of the interferometric phase image detail as it shows the highest IDPC value. The results depicted in Table II, Fig. 5, and Fig. 7 show that the OSMF achieves the same performance when applied to the real interferometric phase image region as it gives the highest value of the ENL and the lowest value of the number of residues.

B. Real Interferogram

The OSMF is applied also to the interferogram of SAR pairs of ERS-1/2 tandem mode single look complex images shown in Fig. 8(a). The filter performance is compared to the three other filters and the results are demonstrated in Table III and Fig. 8.

The results in Table III reveal that the OSMF has excellent reduction of the interferometric image noise as it gives the highest value of the ENL. This is also clear in the smooth areas of the interferometric phase image in Fig. 8(e). The results in Table III show also that the OSMF has the smallest number of residues which means efficient phase unwrapping and hence accurate DEM generation. The results show also that the OSMF achieves perfect preservation of the interferometric phase image detail. This is clear from the perfect reconstruction of the edges of phase fringes demonstrated in Fig. 8(e)

The above discussion verifies that the OSMF achieves an optimum balance between the amount of reduction of the interferometric image noise and the degree of preservation of the phase image detail. This outstanding performance guarantees efficient phase unwrapping and hence accurate DEM generation.

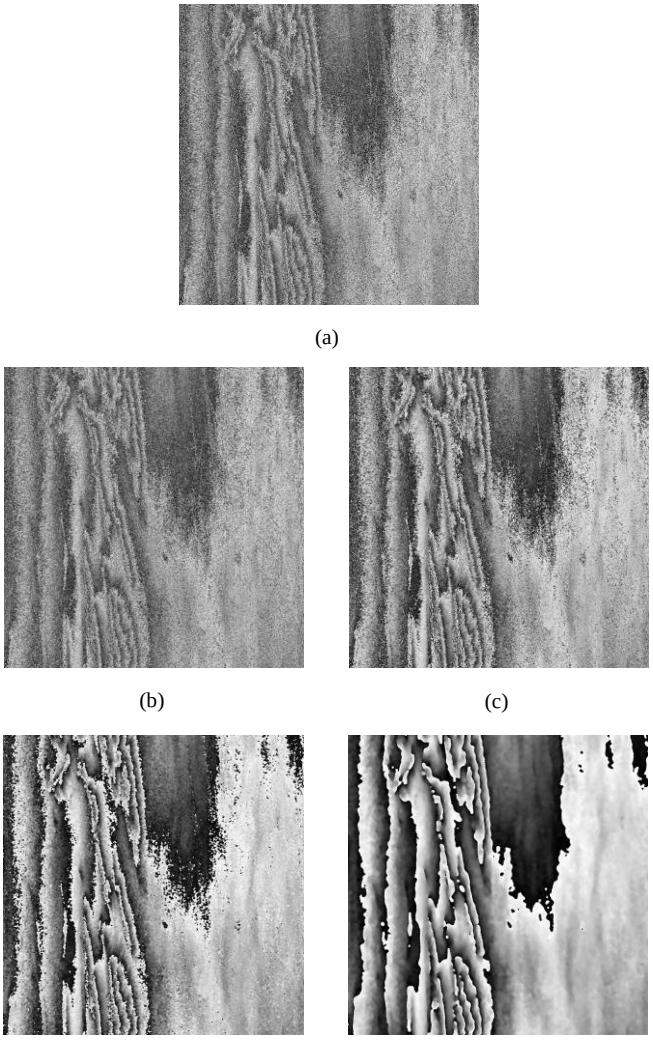

Fig. 8 Filtering results of real interferogram. (a) Noisy. (b) Frost. (c) LAMF. (d) VF. (e) OSMF.

V. CONCLUSION

In this paper, a SMF is proposed to enhance the efficiency of the phase unwrapping process of InSAR phase images and hence improve the accuracy of the generated digital elevation model. The SMF parameters have been optimized using the GA in terms of MAE and IDPC. This is carried out to get an optimum balance between the amount of noise reduction and the degree of detail preservation of the interferometric phase image. The filter performance has been evaluated using simulated and real InSAR interferogram images. The evaluation is based on both objective and subjective measures. The results have been compared to those of other three filters used for filtering the interferometric phase image noise. The results demonstrated that the proposed filter outperformed the other three filters in terms of the objective and the subjective measures.

The results also revealed that the proposed filter achieved high reduction of the interferometric phase image noise with perfect preservation of the image detail and very small number of residues. Hence, the results confirmed that the filter performance guarantees efficient phase unwrapping and consequently accurate DEM generation.

REFERENCES

[1] P. A. Rosen, S. Hensley, I. R. Joughin, F. K. Li, S. N. Madsen, E. Rodriguez and R. M. Goldstein, "Synthetic aperture radar interferometry," *Proc. IEEE*, vol. 88, no. 3, pp. 333-382, 2000.

[2] O. Loffeld, H. Nies, S. Knedlik, and W. Yu, "Phase unwrapping for SAR interferometry—A data fusion approach by Kalman filtering, " *IEEE Trans. Geosci. Remote Sens*., vol. 46, no.1, pp. 47-58, Jan. 2008.

[3] V. S. Frost, J. A. Stiles, K. S. Shanmugan, and J. C. Holtzman, "A model for radar images and its application to adaptive digital filtering of multiplicative noise," *IEEE Trans. Pattern Anal. Mach. Intell*., vol. PAMI-4, no. 2, pp. 157–166, Mar. 1982.

[4] P. Balan, and P. M. Mather. "An adaptive filter for removal of noise in interferometrically derived digital elevation models," *IEEE Geosci. Remote Sens. Symp*., vol. 6, pp. 2529-2531, 2001.

[5] X. Li, H. Song, R. Wang, Y. Shao, and R. Chen, "A patch-based filter for InSAR interferograms, " *IEEE Geosci. Remote Sens. Symp*., pp. 305-308, 2014.

[6] C.-F Chao, K.- Chen, and J.-S Lee, "Refined filtering of interferometric phase from INSAR data," IEEE Trans. Geosci. Remote Sens., vol. 51, no. 12, pp. 5315-5323, Dec. 2013.

[7] F. Qiu, J. Berglund, J. R. Jensen, P. Thakkar, and D. Ren, "Speckle Noise Reduction in SAR Imagery Using a Local Adaptive Median Filter," *GIScience and Remote Sens.*, vol. 41, no. 3, pp. 244-266, 2004.

[8] R. Chen, W. Yu, R. Wang, G. Liu, and Y. Shao "Interferometric phase denoising by pyramid nonlocal means filter," *IEEE Geosci. Remote Sens. Lett*., vol. 10, no. 4, pp. 826-830, Jul. 2013.

[9] W. Feng, V. P. Veronique, M. Sonede, "A vector filtering technique for SAR interferometric phase images," *Proc. IASTED Int. Symp*., *AI*, vol. 566570, 2001.

[10] D. Meng, V. Sethu, E. Ambikairajah, and L. Ge, "A novel technique for noise reduction in InSAR images, " *IEEE Geosci. Remote Sens. Lett*., vol.4 , no. 2, pp. 226-230, April 2007.

[11] X. Lin, F. Li, D. Meng, D. Hu, and C. Ding, "Nonlocal SAR Interferometric Phase Filtering Through Higher Order Singular Value Decomposition," *IEEE Geosci. Remote Sens. Lett*., vol. 12, no. 4, pp. 806-810, Apr. 2015.

[12] Y Bian, and B. Mercer, "Interferometric SAR phase filtering in the wavelet domain using simultaneous detection and estimation," *IEEE Trans. Geosci. Remote Sens*., vol. 49, no. 4, pp. 1396-1416, Apr. 2011.

[13] F. Li, D. Hu, C. Ding, and W. Zhang,"InSAR phase noise reduction based on empirical mode decomposition," *IEEE Geosci. Remote Sens. Lett.*, vol. 10, no. 5, pp.1180-1184, Sep. 2013.

[14] J. Astola and P. Kuosmanen, Fundamentals of Nonlinear Digital Filters. Boca Raton, USA: CRC Press LLC, 1997.

[15] D. E. Goldberg, The Design of Innovation. USA: Kluwer Academic Publishers, 2002.

[16] L. Gomez, M. E. Buemi, J. C. Jacobo-Berlles, and M. E. Mejail,"A new image quality index for objectively evaluating despeckling filtering in SAR images," *IEEE J. Sel. Top. Appl. Earth Obs*., vol. 9, no. 3, pp. 1297-1307, Mar. 2016.